



## NUMERICAL SIMULATION OF CONTROLLED COOLING OF RAILS AS A TOOL FOR OPTIMAL DESIGN OF THIS PROCESS

MACIEJ PIETRZYK<sup>1</sup>, ROMAN KUZIAK<sup>2\*</sup>

<sup>1</sup> AGH University of Science and Technology, Mickiewicza 30, 30-059 Kraków, Poland

<sup>2</sup> Institute for Ferrous Metallurgy, K. Miarki 12, 44-100 Gliwice, Poland

\*Corresponding author: rkuziak@imz.gliwice.pl

### Abstract

The model of controlled cooling of rails is presented in the paper. Model predicts temperature field during cooling, kinetics of phase transformations, microstructural parameters and mechanical properties of the product. Identification of the phase transformation model was performed on the basis of dilatometric tests and inverse analysis. Optimization task was formulated with the objective of searching for the cooling process parameters, which give as low as possible interlamellar spacing in pearlite, microstructure free of bainite and uniform hardness distribution in the rail head. The sensitivity analysis was performed and the following parameters were selected as the optimization variables: time of the 1st stage of fast cooling by immersing in the polymer solution, time of the second stage of cooling in air, depth of the immersion in the polymer solution and heat transfer coefficient between the rail head and the polymer solution.

**Key words:** heat treatment of rails, pearlite, phase transformations modelling, temperature field modelling, mechanical properties

### 1. INTRODUCTION

The constant development of rail transport is specifically connected with an increase in train speed, application of greater axle loads due to an increase in the weight of materials carried by rail transport, as well as linking of the railway networks with the tram infrastructure. Over last decades a constant progress has been observed in the rail transportation sector, which involves implementation of technological solutions complying with the strict safety requirements and regulations imposed on natural environment protection. The rail transport capacities depend strongly on the track parameters. The most important comprise: car stability, geometry of the contact with running wheel, and possibility to sustain greater loads (Kuziak & Zygmunt, 2012). Quality of rails is characterized by the increased abrasive wear strength, fatigue strength and resistance to contact-fatigue defects

occurrence. This features can be obtained for pearlite structure after accelerated cooling with small distance between the cementite lamellae ( $S_0$  around 0.10-0.12  $\mu\text{m}$ ), as compared to the structure after the natural cooling in the air ( $S_0$  around 0.2-0.3  $\mu\text{m}$ ) (Kuziak & Zygmunt, 2012). Reduction of the distance between lamellae results in an increase of pearlite strength/hardness (Kuziak, 1997; Kuziak et al., 1997; Kuziak & Zygmunt, 2012). Simultaneously, it results in thinning of cementite lamellae, which increases plasticity of this phase.

Problem of heat treatment of rails directly after hot rolling has been in the field of interest of scientist for some time. Numerous papers dealing with the phenomena of heat transfer (Ackert & Nott, 1987; Morales et al., 1990; Sahay et al., 2009) microstructure evolution (Perez-Unzueta & Beynon, 1993) and thermal stresses (Boyadiev et al., 1996) can be found

in the scientific literature. Intensive researches aimed at designing of new method of pearlitic rails head hardening process giving rise to substantial progress in reducing of the interlamellar spacing of cementite lamellae and the size of pearlite colony as compared to the these parameters after cooling in still air have been conducted by Kuziak & Zygmunt (2012). Beyond this, various researchers have developed models describing kinetics of phase transformation for eutectoid steels to be adopted into the continuous cooling conditions using additivity rule. These models allow description of such features of the austenite decomposition in eutectoid steels as the transformations start and end temperature and volume fractions of structural components. More advanced models can predict such specific features of the pearlitic microstructure as grain size, colony size and interlamellar spacing, see for example Authors paper (Pietrzyk & Kuziak, 2000). Accuracy of these models was limited due to number of parameters, which were difficult to determine. Significant progress in experimental techniques during last decade created a possibility of identification of parameters in microstructure evolution models for eutectoid steels. Therefore, the objective of the present work was identification of the parameters in microstructure evolution models for eutectoid steels using physical simulation of the cooling process combined with the inverse analysis. Experiments performed in IMŻ Gliwice supplied the data for identification. Direct problem model was based on the FE solution for cooling of rails. Microstructure evolution equations were implemented in the FE code and they were solved in each Gauss integration point. Inverse analysis was applied for identification of coefficients in the model. Developed model was tested in simulations of controlled cooling of rails on the semi industrial cooling system.

## 2. MICROSTRUCTURE EVOLUTION AND MECHANICAL PROPERTIES MODELS FOR EUTECTOID STEELS

The models, which will be used in optimization of the controlled cooling of rails, are divided into phase transformation models, microstructure models and mechanical properties models. These three models are described below.

### 2.1. Phase transformation model

Detailed description of this model can be found in (Pietrzyk & Kuziak, 2000). This model with slight

modifications is described briefly below. The model for pearlitic and bainitic transformations is based on JMAK (Johnson, Mehl, Avrami, Kolmogorov) type equation:

$$X = 1 - \exp(-kt^n) \quad (1)$$

where:  $X$  – transformed volume fraction,  $k$ ,  $n$  – coefficients,  $t$  – time.

In this approach, all attention is focused on the kinetics and microstructural aspects are essentially ignored. However, even in the simplest JMAK model, nucleation and growth are recognized as being the two relevant and intrinsically different processes. Scheil (1935) additivity rule has to be applied in this model to account for the temperature changes during transformations. Incubation time for pearlitic and bainitic transformation is accounted for.

$$\text{pearlite: } \tau_p = \frac{a_1}{(Ae_1 - T)^{a_3}} \exp\left[\frac{a_2 \times 10^3}{R(T + 273)}\right] \quad (2)$$

$$\text{bainite: } \tau_b = \frac{a_9}{(a_{12} - T)^{a_{11}}} \exp\left[\frac{a_{10} \times 10^3}{R(T + 273)}\right] \quad (3)$$

where:  $T$  – temperature in °C,  $R$  – gas constant.

Theoretical considerations show that, according to transformation type (nucleation and growth, site saturation) a constant value of coefficient  $n$  in equation (1) can be used. The values of  $n$  are introduced in the model as  $a_4$  and  $a_{13}$  for pearlitic and bainitic transformations, respectively. Coefficient  $k$  should map the form of a TTT diagram. Following that observation, the  $k$  is defined as a temperature function  $k = f(T)$ . This function has to be flexible enough to replicate complex phenomena of nucleation and growth controlled by diffusion, interface mobility and solute-drag effect. The following function is proposed:

$$\text{pearlite: } k = \frac{a_7}{D^{a_8}} \exp\left(a_6 - \frac{a_5 T}{100}\right) \quad (4)$$

$$\text{bainite: } k = a_{17} \exp\left(a_{16} - \frac{a_{15} T}{100}\right) \quad (5)$$

where:  $D$  – grain size.

Remaining equations in the model are:

– Start temperature for bainitic transformation:

$$B_s = a_{13} - 425[\text{C}] - 42.5[\text{Mn}] - 31.5[\text{Ni}] \quad (6)$$

– Start temperature for martensitic transformation:



$$M_s = a_{18} - a_{19}c_\gamma \quad (7)$$

Fraction of the austenite, which transforms into the martensite, is calculated according to the model of Koistinen and Marburger (1959), described also in (Umamoto et al., 1992; Pietrzyk et al., 2003):

$$X_m = 1 - \exp[-0.011(M_s - T)] \quad (8)$$

Equation (8) represents volume fraction of martensite with respect to the volume of austenite, which was remaining at the temperature  $M_s$ . The volume fraction of martensite with respect to the whole volume of the material is:

$$F_m = (1 - F_p - F_b) X_m \quad (9)$$

where:  $F_p$ ,  $F_b$  – volume fractions of pearlite and bainite with respect to the whole volume of the sample.

## 2.2. Microstructure model

The model includes equations, which describe microstructural parameters of eutectoid steel after cooling from austenite stability temperature to the room temperature. Pearlitic transformation involves the nucleation and growth process of pearlite nuclei. Nucleation primarily occurs at corners, edges and surfaces of austenite grain boundaries. The resulting microstructure is composed of pearlite nodes subdivided into colonies in the process of pearlite growth. Typically, there are several colonies in pearlite grains, characterized by parallel orientation of the cementite/ferrite lamellae within each colony (figure 1a), where definitions of pearlite grain size ( $D_p$ ) and colony size ( $D_c$ ) are given. High or low angle boundaries can develop between neighbouring pearlite colonies during the transformation.

Such pearlite microstructure is formed when austenite grains before the transformation are relatively large ( $\geq 20 \mu\text{m}$ ), and pearlitic transformation occurs with minor undercooling with respect to the temperature  $Ae_1$ . For smaller austenite grains and considerable undercooling of austenite at the beginning of transformation, the difference between the nodes and pearlite colonies disappears. In such a situation, steel structure contains pearlite colonies only and such pearlite was called a colonial pearlite by Garbarz and Pickering (1988).

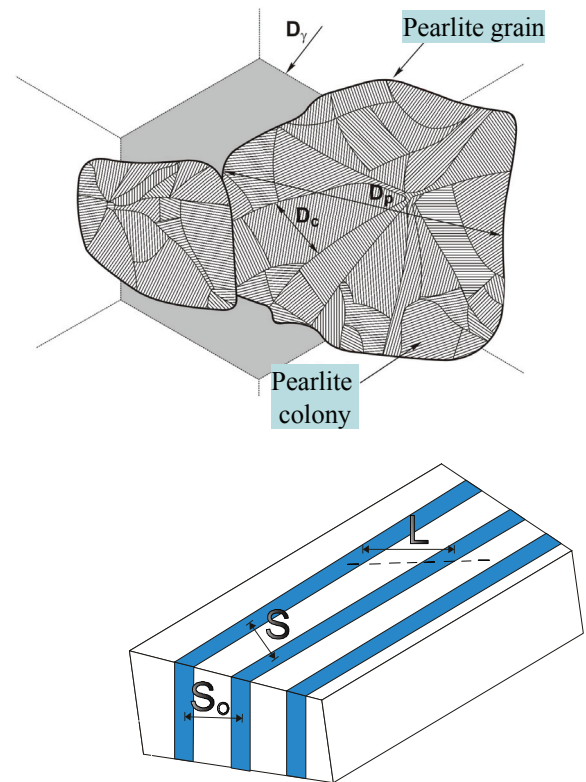


**Fig. 1.** Parameters of microstructure in pearlite: a)  $D_\gamma$  - former austenite grain,  $D_p$  - pearlite grain,  $D_c$  - pearlite colony; b)  $S_0$  - interlamellar spacing,  $S$  - interlamellar spacing in the plane of observation,  $L$  - average secant.

The spacing between cementite lamellae is the most important parameter characterizing pearlite microstructure. Schematic definition of this parameter is given in figure 1 (Kuziak & Zygmunt, 2012), presenting the interrelation between the actual distance between the cementite lamellae –  $S_0$ , interlamellar spacing in the plane of observation –  $S$ , and measured mean linear intercept of cementite lamellae –  $L$ .

The surface layer of rail head is of particular interest. Fine pearlite should be a dominant component of this layer. The interlamellar spacing in pearlite, in  $\mu\text{m}$ , is calculated as:

$$S_0 = \frac{1}{a - bT_p} \quad (10)$$

$$a = 129.3 - 54.4[\text{Mn}] - 4.38[\text{Cr}] - 17.5[\text{Si}]$$

$$b = 0.178 - 0.072[\text{Mn}] - 0.012[\text{Cr}] - 0.0274[\text{Si}]$$

where:  $T_p$  – temperature of pearlitic transformation in  $^\circ\text{C}$ ,  $[\text{Mn}]$ ,  $[\text{Cr}]$ ,  $[\text{Si}]$ ,  $[\text{C}]$  – manganese, chromium, silicon and carbon content in wt%.

Since the temperature varies during cooling, the interlamellar spacing is calculated for weighted average temperature during the transformation. Pearlite grain size ( $D_p$ ) and pearlite colony size ( $D_c$ ) are two



additional parameters included in the model. They are calculated from the following equations (Pietrzyk & Kuziak, 2000):

$$D_p = \frac{6500 \left[ 1 - \exp(-0.016D_\gamma) \right]^{0.6}}{Ae_1 - T_p} \quad (11)$$

$$D_c = \frac{1}{0.857 - 0.00119T_p} \quad (12)$$

where:  $T_p$  – average temperature of pearlitic transformation in °C.

### 2.3. Mechanical properties model

The equations, which describe mechanical properties of eutectoid steel in the room temperature, are included in the model, as well. Yield stress ( $R_{0.2}$ ) and tensile strength ( $R_m$ ) in MPa for eutectoid steel are calculated as (Kuziak & Zygmunt, 2013):

$$R_{0.2} = 259 + 0.087\chi^{-1}$$

$$R_m = 793 + 0.07\chi^{-1} + 122[\text{Si}] \quad (13)$$

where:  $\chi = (2S_0 - t)$  - the mean free path for dislocation glide in pearlitic ferrite,  $t$  – thickness of the cementite plate calculated as  $0.015S_0[\text{C}], [\text{Si}], [\text{C}]$  – silicon and carbon content in wght%.

According to Kuziak & Zygmunt (2013), temperature of pearlitic transformation in naturally cooled rails is within the range of around 690-670°C, which allows to achieve  $R_m$  in the range of 850-900 MPa. To achieve strength higher than 1200 MPa, pearlitic transformation should occur below 560°C.

The wear resistance of pearlitic rails is directly linked with their hardness. Increasing the hardness causes the wear resistance increase. The Brinell hardness can approximately be calculated as  $HB = 0.3R_m$  (Kuziak & Zygmunt, 2013).

### 3. IDENTIFICATION OF THE PHASE TRANSFORMATION MODEL

The chemical composition of experimental steel grade 900A was as follows: 0.71%C, 1.1%Mn,

0.25%Si, and 0.13%Cr. ThermoCalc software was used to determine equilibrium carbon concentrations. The following relations were obtained for the investigated steel:

$$c_{\gamma\beta} = -1.46583 + 0.002887T$$

$$c_{\gamma\alpha} = 4.8513 - 0.005776T \quad (14)$$

where:  $c_{\gamma\alpha}$  - carbon content at the  $\gamma/\alpha$  interface,  $c_{\gamma\beta}$  - carbon content at the  $\gamma/\text{cementite}$  interface,  $T$  - temperature in °C.

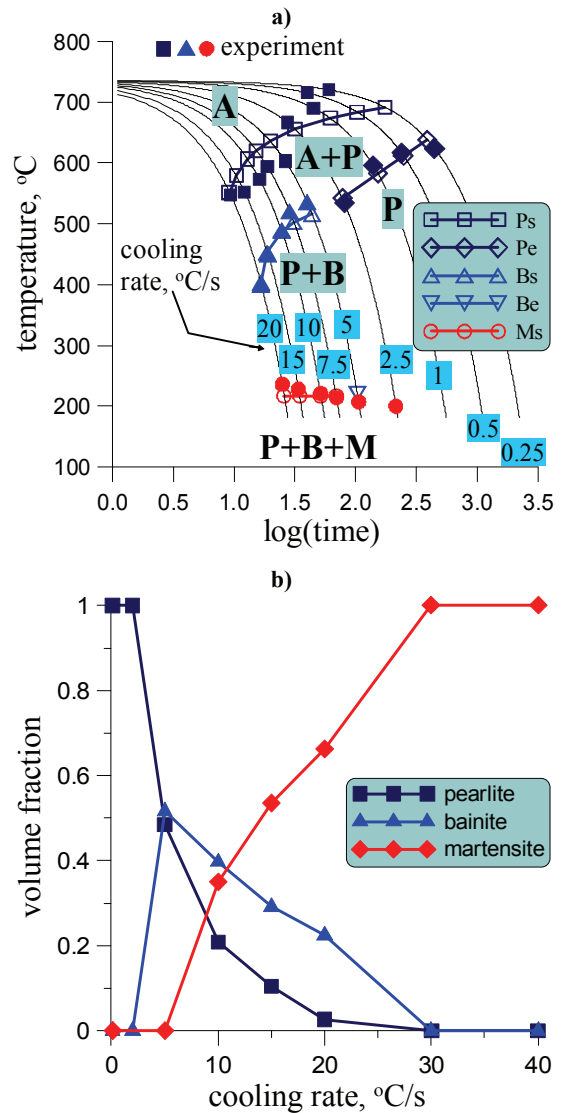


Fig. 2. a) Comparison of the predictions of the phase transformation model (coefficients in table 1) with measurements for the transformations start and end temperatures; b) Results of calculations of volume fractions of phases for various cooling rates.

Table 1. Coefficients in the phase transformation model determined using inverse analysis of the dilatometric tests.

$a_1$	$a_2$	$a_3$	$a_4$	$a_5$	$a_6$	$a_7$	$a_8$	$a_9$	$a_{10}$
0.0779	122.8	2.634	0.0632	0.134	8.913	0.013	0.862	1399	61.98
$a_{11}$	$a_{12}$	$a_{13}$	$a_{14}$	$a_{15}$	$a_{16}$	$a_{17}$	$a_{18}$	$a_{19}$	
2.537	887.6	1.083	887.6	0.942	0.399	0.386	218.1	1.646	





Dilatometric tests were performed for the investigated steel. Inverse analysis was applied to identify coefficients  $\mathbf{a} = \{a_1, \dots, a_{19}\}$  for this steel. Inverse algorithm proposed first for plastometric tests (Szeliga et al., 2006) and applied by Pietrzyk et al. (2000) and by Pietrzyk & Kuziak (2012) to dilatometric tests for carbon-manganese steels, was used in the present work for eutectoid steels. Coefficients  $\mathbf{a}$  determined for the investigated steel 900A are given in table 1. Comparison between measured and calculated start and end temperatures for phase transformations are given in figure 2a. Reasonably good agreement between predictions and measurements was obtained. Some discrepancies are observed for the start temperature for the pearlitic transformation but they are probably due to scatter of the experimental data. Results of calculations of volume fractions of phases for various cooling rates are shown in figure 2b.

#### 4. COMPUTER AIDED DESIGN OF THE COOLING TECHNOLOGY

A new method of rail head hardening of standard-gauge rails proposed by Kuziak & Zygmunt (2013) was considered. Obtaining of improved wear and damage resistance of the rail head was the objective of the new technology. Application of numerical simulations to design of the cooling technology, which gives the required microstructure, is described in this chapter.

##### 4.1. New rail cooling technology

The general requirements concerning microstructure of the rail are as follows:

- Purely pearlitic microstructure at the whole cross section of the rail, without martensite or bainite,
- As small as possible interlamellar spacing in the rail head,
- Uniform distribution of hardness at the cross section of the rail head.

On the basis of tests performed on Gleeble 3800 it was shown by Kuziak and Zygmunt (2013) that the optimal relation between strength and ductility for eutectoid steel was obtained after isothermal holding at 550°C. The pearlite microstructure after holding at this temperature is composed of fine pearlite having interlamellar spacing around 0.11  $\mu\text{m}$  and colony size of 8  $\mu\text{m}$ . When the pearlitic transformation occurs at lower temperature range,

the structure contains, besides lamellar pearlite, degenerated pearlite and bainite. When austenite decomposition occurs at temperature below 500°C, mainly bainite is present in the microstructure. Increase in the volume fraction of degenerated pearlite and bainite in rail structure reduces its ductility.

On the basis of these observations Kuziak & Zygmunt (2013) developed a cyclic immersion hardening of the rail head, which enables a homogeneous hardness to be achieved in the rail head, without the necessity of accurate control of the total time of heat treatment. The rail is inserted in the tank with the coolant directly after rolling, and initially the level of the solution is kept below the running surface level. The process of accelerated cooling starts when the rail head temperature reaches about 820°C. Then the pumps supply the solution to the tank, which leads to gradual immersion of the rail head (figure 3a). Keeping the head immersed for a longer period of time would lead to occurrence of the bainite in the microstructure. Therefore, the head is immersed cyclically into the polymer solution for short periods of time, after which part of the solution is removed from the tank, which brings its level below the running surface of the head (figure 3b)

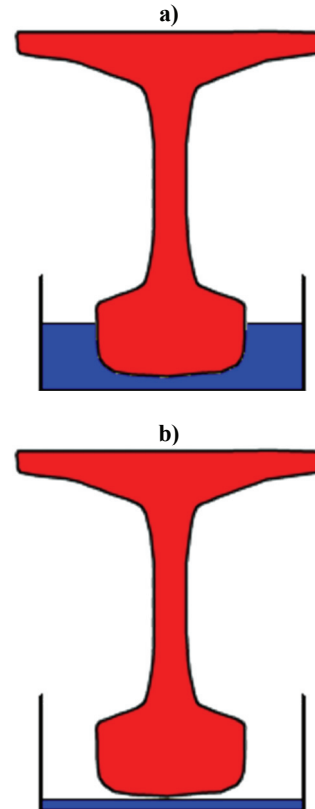


*Fig. 3. a) Schematic illustration of one stage of controlled cooling of rail head, a) head immersed in the solution, b) head above the level of the solution.*



and the rate at which heat is transferred to the environment from the head is substantially reduced. At this stage transfer of heat from the hotter rail head centre increases the temperature of the running surface. For the proper performance of the head hardening process, it is critical for the running surface temperature not to increase above  $570^{\circ}\text{C}$ . To prevent this, the coolant level is raised in the tank again and accelerated cooling stage is repeated. Sequence “accelerated cooling – cooling in still air can be repeated many times until the pearlite transformation is completed in the entire head. Proper selection of times is crucial to maintain low temperature of pearlitic transformation and to avoid danger that the running surface is cooled below the start temperature of the bainitic transformation prior to the pearlitic transformation completion.

#### 4.2. Simulation of controlled cooling of rail head

Temperature distribution calculated at 5 s after the exit from the last pass is shown in figure 4a and the finite element mesh used in simulations of controlled cooling is shown in figure 4b. After trial and error method the cooling cycle composed of 30 s immersion in the solution followed by 30 s in air and further cooling in the solution was selected for numerical tests. A gradual rail's head immersion and lowering the level of solution was assumed in the simulations. The heat transfer coefficient for the steel immersed in the polymer solution was determined in the earlier not published experiments. The value of this coefficient was  $1700\text{ W/m}^2\text{K}$  at surface temperatures exceeding  $700^{\circ}\text{C}$ . When temperature was decreasing below  $700^{\circ}\text{C}$  the heat transfer coefficient was increasing and reached the maximum value of  $2400\text{ W/m}^2\text{K}$  at  $300^{\circ}\text{C}$ . Further decrease of the temperature resulted in the decrease of the heat transfer coefficient to the value of  $1200\text{ W/m}^2\text{K}$  at the room temperature. Results of simulations of the controlled cooling process for rails are shown in figures 5 and 6.

Time-temperature profiles at 4 locations shown in figure 4b are presented in figure 5a. It is seen in this figure that during cooling in air temperature at points located close to the head surface is increasing, due to heat transfer from the hotter centre of the head. Kinetics of phase transformations is shown in figure 5b. Since for the considered cooling cycle purely pearlitic microstructure was obtained at the

whole cross section of the rail, the results for the location D only are presented in this figure.

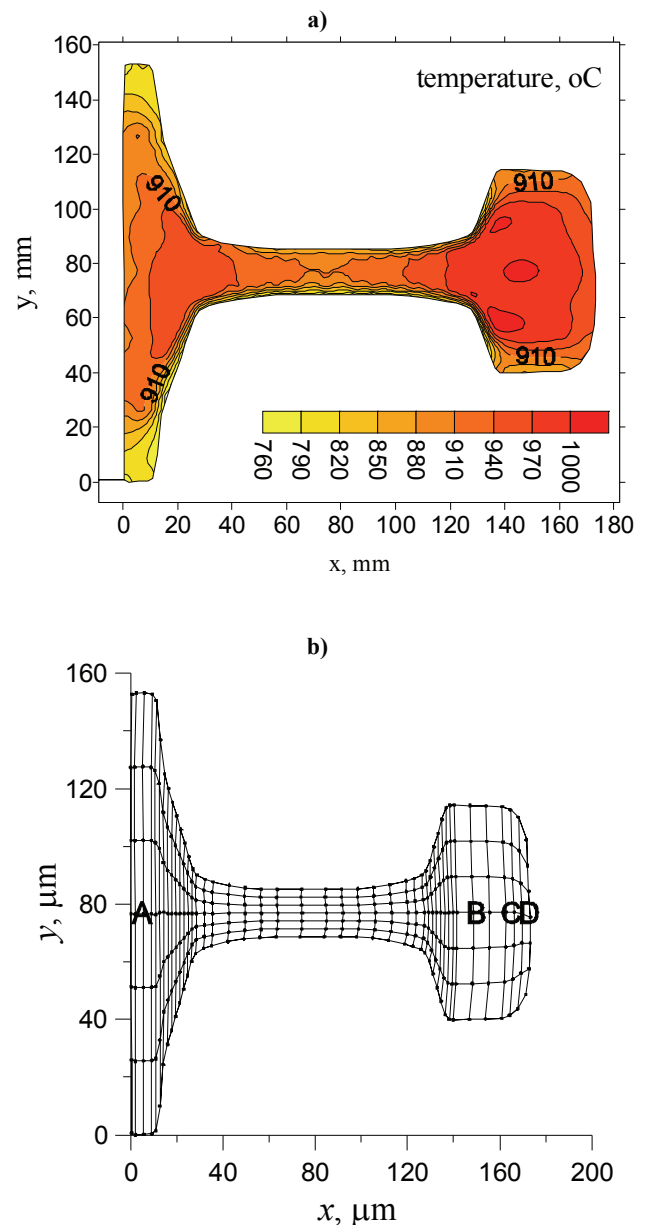


Fig. 4. a) Temperature distribution in the rail 5 s after exit from the last pass, b) Finite element mesh used in simulations of controlled cooling.

Distributions of microstructural parameters at the rail cross section after cooling cycle are shown in figure 6. As expected, the finest microstructural parameters were obtained in the rail head. The colony size below  $8\ \mu\text{m}$  suggested by Kuziak & Zygmunt (2013) was achieved in the rail head. On the other hand, the required value of  $0.11\ \mu\text{m}$  for interlamellar space was not obtained, what means that further improvement of the cooling cycle parameters is necessary.



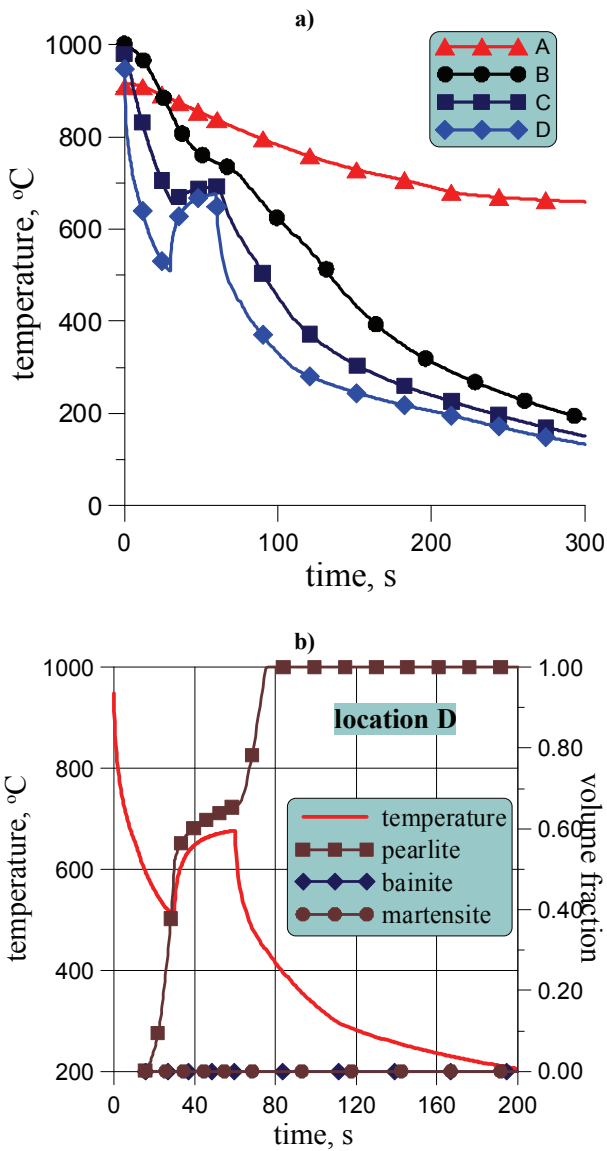


Fig. 5. a) Time-temperature profiles at 4 locations shown in figure 4b, b) Kinetics of phase transformations at location D.

Distributions of mechanical properties at the cross section of the rail are shown in figure 7. Following the microstructural parameters, the highest mechanical properties were obtained for the rail head. Yield stress and yield stress are heterogeneous, increase of these parameters close to the surface was observed. Heterogeneity of the hardness is lower but still significant. It may be concluded that further search for the cooling parameters, which will give more homogeneous properties, is needed.

Recapitulating the research described above it can be concluded that numerical modelling can predict various microstructural and mechanical parameters in the rails depending on the cooling schedule. Therefore, this method can be used in the design of the optimal cooling parameters. The optimization task for the cooling of rails is formulated in the fol-

lowing part of the paper. It is preceded by the sensitivity analysis.

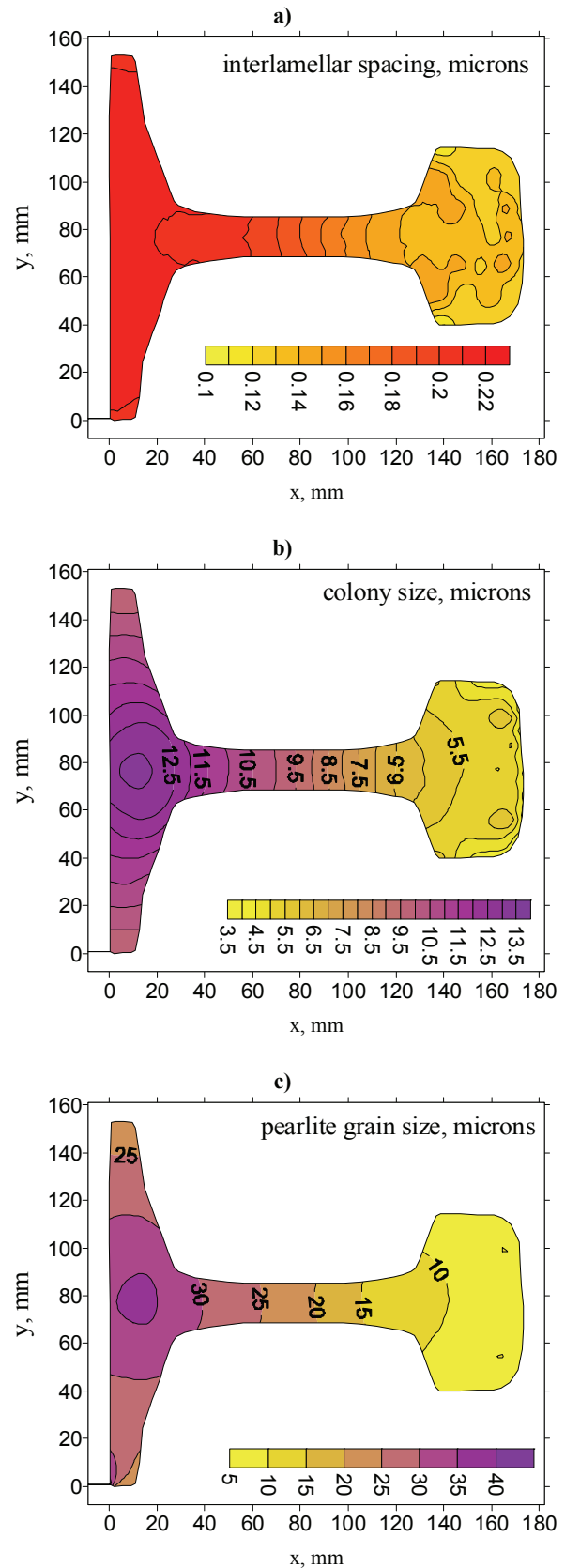


Fig. 6. Calculated distribution of the interlamellar spacing (a), pearlite colony size (b) and pearlite grain size (c) at the cross section of the rail after the cooling cycle.



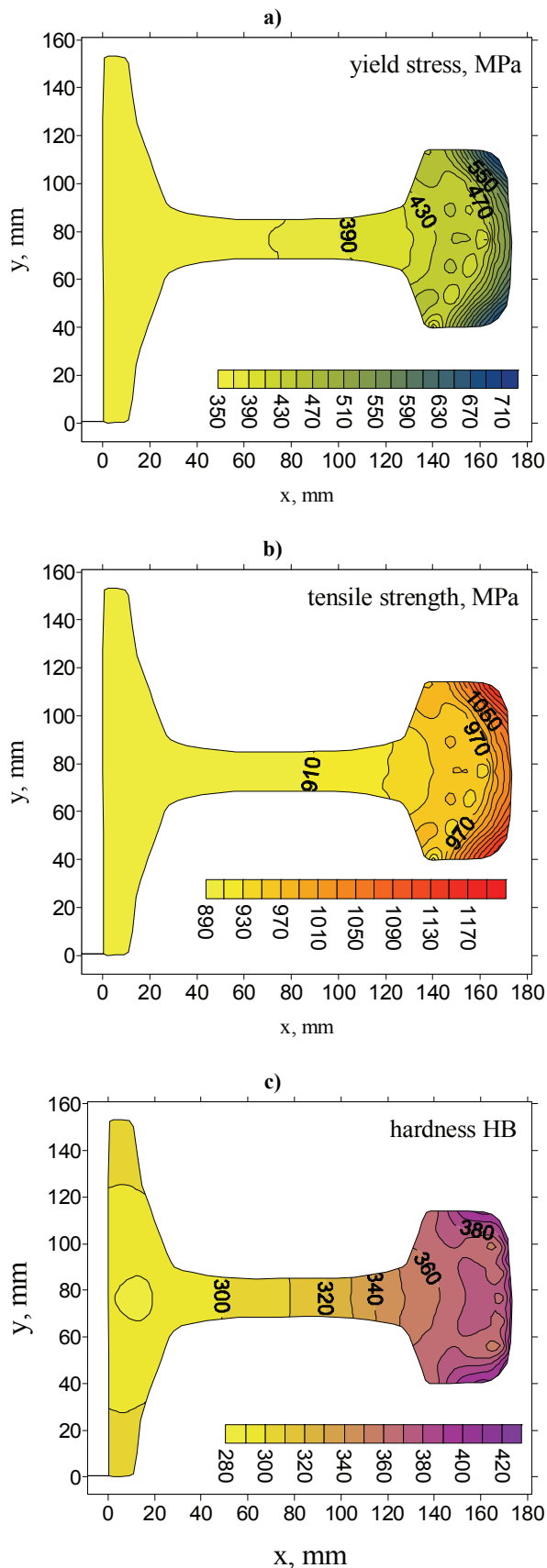


Fig. 7. Calculated distribution of the yield stress (a), yield strength (b) and hardness HB (c) at the cross section of the rail after the cooling cycle.

### 4.3. Optimization task

In the case of controlled cooling of rails the goal of the optimization is to obtain the product with the following features (for the rail head):

- as low as possible interlamellar space,
- lack of bainite,
- uniform distribution of hardness.

These are not conflicting goals, therefore, the following objective function was proposed:

$$\Phi = \sqrt{\sum_{i=1}^{n_{gp}} \left( \frac{HB_i - HB_{ave}}{HB_i} \right)^2 + \sum_{i=1}^{n_{gp}} (S_{01}^2 + F_{bi}^2)} \quad (15)$$

where:  $HB_{ave}$  – the average hardness of the rail head,  $n_{gp}$  – number of Gauss integration points in the rail head.

The goal of the present work was to select the cooling process parameters, which have the largest influence on the objective function. This goal was reached by performing the sensitivity analysis. The parameters selected after the sensitivity analysis will become the optimization variables.

### 4.4. Sensitivity analysis

Sensitivity analysis (SA) methods were applied to estimate the effect of various parameters of the cooling process on the output, which is the objective function in optimization. SA determines the parameters contributing the most to the output variability. It also indicates the parameters that are insignificant and that may be eliminated from the optimization. Moreover, the sensitivity analysis evaluates the parameters, which interact with each other and determines the input parameters region for subsequent calibration space. Performing SA requires to define the following terms (Kleiber et al., 1997, Szeliga, 2011; Szeliga, 2012):

- *Objective function measure.* The measure expresses the objective function as a scalar value.
- *Selection of the parameter domain points.* Design of experiment techniques to be used to select the lower number of points guaranteeing searching the whole parameters domain.
- *Sensitivity measure.* The sensitivities, defined as global or local indices, are estimated based on the objective function measure variations caused by the process parameters changes.

The sensitivity analysis was applied to evaluate the influence of the cooling process parameters on the objective function (15). The Morris (1991) algo-





rithm was applied. This method gives qualitative information on the objective function sensitivity with respect to the technological parameters. Morris one-at-a-time Design belongs to the group of screening methods. In this algorithm the elementary effect  $\zeta_i$  is introduced to calculate the sensitivities:

$$\xi_i(\mathbf{x}) := \frac{\Phi(x_1, \dots, x_{i-1}, x_i + \Delta_i, x_{i+1}, \dots, x_k) - \Phi(\mathbf{x})}{\Delta_i} \quad (16)$$

where:  $\mathbf{x} \in \Omega \subset P^k$  - the  $k$ -dimensional vector of process parameters  $x_i$ ,  $\Omega$  - domain of the analysis, which was the rail head,  $\Delta_i$  - increment of the  $i$ th parameter.

In the first approach to the sensitivity analysis the following four parameters of the cooling process were selected as the independent variables:  $t_1$  - time of the first stage of accelerated cooling (head immersed in the solution),  $t_2$  - time of the first stage of air cooling,  $d$  - depth of the immersion of the head in the solution,  $h$  - the heat transfer coefficient represented in the analysis by its maximum value. The depth  $d$  can be changed by control of the pouring of the polymer solution into the tank. The heat transfer coefficient can be changed by changing the concentration of the solution. It was assumed that when the maximum value of  $h$  is increased/decreased, the whole plot  $h(T)$  is moved up/down.

To obtain more detailed information regarding influence of the independent variables the sensitivity of each part of the objective function (15) was calculated separately. Thus, instead of the whole objective function  $\Phi$  in equation (15), three dependent variables were selected, the average interlamellar spacing ( $S_0$ ), the average volume fraction of bainite ( $F_b$ ) and the homogeneity factor for the hardness ( $\Delta HB$ ):

$$\Delta HB = \sqrt{\sum_{i=1}^{n_{gp}} \left( \frac{HB_i - HB_{ave}}{HB_i} \right)^2} \quad (17)$$

All three dependent variables were calculated for the  $\Omega$ , which was the rail head. A finite distribution of elementary effects  $\zeta_i$  calculated for the  $i$ th factor was found by sampling  $\mathbf{x}$  in  $\Omega$ . Based on that distribution, expected value  $\mu_i$  and standard deviation  $\sigma_i$  for  $i$ th model parameter were estimated through the classic estimators for independent random samples. Since elementary effects  $\zeta_i$  are sensitive to the parameter disturbance  $\Delta_i$ , finite distribution of  $\zeta_i$  is estimated with various values of  $\Delta_i$ . To compare the results of means  $\mu_i$  and standard deviations  $\sigma_i$  esti-

mations obtained for various  $\mathbf{x}$  and  $\Delta_i$  are normalized:

$$\bar{\mu}_i = \frac{\mu_i}{\|\boldsymbol{\mu}\|} \quad \bar{\sigma}_i = \frac{\sigma_i}{\|\boldsymbol{\sigma}\|} \quad (18)$$

Results of calculations of sensitivity coefficients  $\bar{\mu}_i$  and standard deviations  $\bar{\sigma}_i$  are shown in figure 8. It is seen in this figure that volume fraction of bainite is sensitive to all considered variables. Standard deviations for these variables are large, what means that relation of the bainite volume fraction with the optimization variables is nonlinear. Slightly lower but still noticeable sensitivities were obtained for the interlamellar spacing. It can be concluded that all four independent variables will be effective in optimization of the bainite content and interlamellar spacing. Contrary, negligible sensitivity of the bainite homogeneity with respect to the independent variables was obtained. It means that it would be difficult to control homogeneity of hardness in the rail head. On the other hand, reasonably uniform hardness distribution was obtained for all investigated cases, see figure 7c.

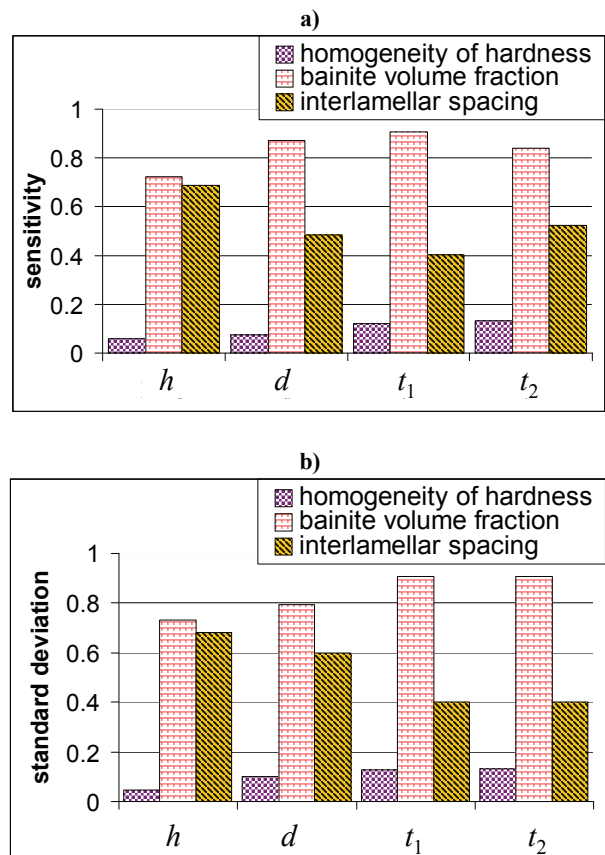


Fig. 8. Sensitivity coefficients (a) and standard deviations (b) calculated for four optimization variables and three dependent variables.



## 5. CONCLUSIONS

The model of controlled cooling of rails was presented in the paper. Model predicts temperature field during cooling, kinetics of phase transformations, microstructural parameters and mechanical properties of the product. Optimization task was formulated with the objective of searching for the cooling process parameters, which give uniform hardness distribution, as low as possible interlamellar spacing in pearlite in the rail head and free of bainite microstructure in the whole rail. The sensitivity analysis was performed and the following conclusions were drawn:

- Four parameters of the cooling process were selected as the independent variables in the optimization: heat transfer coefficient for cooling in the polymer solution, depth of immersion of the rail head, time of fast cooling in the polymer solution and time of cooling in the air at the second stage of cooling.
- Volume fraction of bainite is sensitive to all considered optimization variables. Standard deviations for these variables are large, what means that relation of the bainite volume fraction on the optimization variables is nonlinear.
- Slightly lower but still noticeable sensitivities were obtained for the interlamellar spacing.
- All selected independent variables will be effective in optimization of the bainite content and interlamellar spacing.
- Sensitivity of the bainite homogeneity with respect to the independent variables was negligible. It means that control of hardness homogeneity in the rail head would be difficult. On the other hand, reasonably uniform hardness distribution at the cross section of the rail head was obtained for all investigated cases.

Further research should focus on including additional properties of rails into optimization. The fatigue resistance and wear resistance of the rail head surface in contact with wheels has to be considered next.

**Acknowledgements.** Financial assistance of the AGH project no. 11.11.110.080 is acknowledged.

## REFERENCES

Ackert, R.J., Nott, M.A., 1987, Accelerated water cooling of railway rails in-line with the hot rolling mill, *Proc. Symp. Accelerated Cooling of Rolled Steels*, eds, Ruddle,

G.E., Crawley, A.F., Pergamon Press, Winnipeg, 359-372.

- Boyadiev, I.I., Thomson, P.F., Lam, Y.C., 1996, Computation of the diffusional transformation of continuously cooled austenite for predicting the coefficient of thermal expansion in the numerical analysis of thermal stress, *ISIJ International*, 36, 1413-1419.
- Garbarz, B., Pickering, F.B., 1988, Effect of pearlite morphology on impact toughness of eutectoid steel containing vanadium, *Materials Science and Technology*, 4, 328-334.
- Kleiber, M., Antunez, H., Hien, T.D., Kowalczyk, P., 1997, *Parameter Sensitivity in Nonlinear Mechanics*, Wiley.
- Koistinen, D.P., Marburger, R.E., 1959, A general equation prescribing the extent of the austenite-martensite transformation in pure iron-carbon alloys and plain carbon steels, *Acta Metallurgica*, 7, 59-69.
- Kuziak, R., 1997, Matematyczne modelowanie zmian mikrostrukturalnych podczas nagrzewania, przerobki cieplno-plastycznej i chłodzenia stali perlitycznych, *Prace IMZ*, 49, 3-54 (in Polish).
- Kuziak, R., Cheng, Y.-W., Głowacki, M., Pietrzyk, M., 1997, Modelling of the microstructure and mechanical properties of steels during thermomechanical processing, *NIST Technical Note 1393*, Boulder.
- Kuziak, R., Zygmunt, T., 2013, A new method of rail head hardening of standard-gauge rails for improved wear and damage resistance, *Steel Research International*, 84, 13-19.
- Morales, R.D., Lopez, A.G., Olivares, I.M., 1990, Heat transfer analysis during water spray cooling of steel rods, *ISIJ International*, 30, 48-57.
- Morris, M.D., 1991, Factorial sampling plans for preliminary computational experiments, *Technometrics*, 33, 161-174.
- Perez-Unzueta, A.J., Beynon, J.H., 1993, Microstructure and wear resistance of pearlitic rail steels, *Wear*, 162-164, 173-182.
- Pietrzyk, M., Kuziak, R., 2000, Modeling of controlled cooling of rails after hot rolling, *Proc. Conf. Rolling 2000*, Vasteros, CD ROM.
- Pietrzyk, M., Kondek, T., Majta, J., Zurek, A.K., 2000, Method of identification of the phase transformation model for steels, *Proc. COM 2000*, Ottawa, CD ROM.
- Pietrzyk M., Kuziak R., Kondek T., 2003, Physical and numerical modelling of plastic deformation of steels in two-phase region, *Proc. 45th MWSP Conf.*, Chicago, 209-220.
- Pietrzyk, M., Kuziak, R., 2012, Modelling phase transformations in steel, in: *Microstructure evolution in metal forming processes*, (eds), Lin, J., Balint, D., Pietrzyk, M., Woodhead Publishing, Oxford, 145-179.
- Sahay, S.S., Mohapatra, G., Totten, G.E., 2009, Overview of pearlitic rail steels: accelerated cooling, quenching, microstructure and mechanical properties, *Journal of ASTM International*, 6, 1-26.
- Scheil, E., 1935, Anlaufzeit der Austenitumwandlung, *Archiv für Eisenhüttenwesen*, 12, 565-567.
- Szeliga, D., Gawąd, J., Pietrzyk, M., 2006, Inverse Analysis for Identification of Rheological and Friction Models in Metal Forming, *Computer Methods in Applied Mechanics and Engineering*, 195, 6778-6798.
- Szeliga, D., 2011, Application of sensitivity analysis – preliminary step of the process parameters estimation. *Proc. XI Conf. COMPLAS*, (eds), Oñate, E., Owen, D.R.J., Peric, D., Suarez, B., Barcelona, 1359-1367, (e-book).



- Szeliga, D., 2012, Selection of the appropriate phase transformation model for design of laminar cooling and continuous annealing of DP steels, *Computer Methods in Materials Science*, 12, 70-84.
- Umamoto, M., Hiramatsu, A., Moriya, A., Watanabe, T., Nanba, S., Nakajima, N., Anan, G., Higo, Y., 1992, Computer modelling of phase transformation from work-hardened austenite, *ISIJ International*, 32, 306-315.

## NUMERYCZNA SYMULACJA KONTROLOWANEGO CHŁODZENIA SZYN JAKO NARZĘDZIE WSPOMAGAJĄCE PROJEKTOWANIE TEGO PROCESU

### Streszczenie

W pracy opisano model kontrolowanego chłodzenia szyn po walcowaniu. Model oblicza pole temperatury w czasie chłodzenia oraz kinetykę przemian fazowych, parametry mikrostruktury po ochłodzeniu do temperatury otoczenia i własności mechaniczne gotowego wyrobu. Identyfikację modelu przemian fazowych przeprowadzono na podstawie prób dylatometrycznych i analizy odwrotnej. Zadanie optymalizacyjne dla procesu chłodzenia zostało sformułowane jako poszukiwanie parametrów tego procesu, które dają najmniejsze wartości odległości między płytkami cementytu w perlacie, brak bainitu w całej objętości szyny i równomierny rozkład twardości na przekroju główki szyny. Przeprowadzono analizę wrażliwości składowych funkcji celu względem zmiennych optymalizacji i na tej podstawie wybrano 4 zmienne do dalszej analizy: czas przyspieszonego chłodzenia w pierwszym etapie przez zanurzenie w roztworze polimerowym, czas swobodnego chłodzenia w powietrzu w drugim etapie, głębokość zanurzenia główki szyny w roztworze oraz współczynnik wymiany ciepła między powierzchnią szyny i roztworem.

*Received: January 10, 2013*

*Received in a revised form: January 29, 2013*

*Accepted: January 31, 2013*

